CHAPTER 143

SHEAR INSTABILITY OF LONGSHORE CURRENTS: EFFECTS OF DISSIPATION AND NON-LINEARITY

Albert Falqués, Vicente Iranzo and Miquel Caballería [1]

Abstract

The effect of bottom friction and turbulent lateral mixing on shear instability of the longshore current is investigated. Transition conditions for this instability as a function of non-dimensional parameters related to the basic current, topography, bottom friction and lateral mixing are found. A direct nonlinear numerical simulation of shear instability is presented. The basic flow is found to be supercritical and the amplitude of shear waves can reach at least 20% of the basic flow. A small increase in the period due to non-linearity is also found. Preliminary results suggest that far from criticality there is an important contribution of the instability to the mean flow. Some applications to field and laboratory experiments are discussed.

1. Introduction

In the presence of a significant wave-driven longshore current, low frequency oscillations in the current that are not due to gravity waves may appear. These oscillations, called far infragravity waves (FIG waves) because their frequency is lower than the infragravity edge waves of the same wavenumber, were first observed by Oltman-Shay et al. (1989) as strong fluctuations in the time series of longshore and cross-shore velocity components. They appear as a meandering in the current that propagates downflow. According to the spectral analysis performed by Oltman-Shay and co-workers, they are almost non-dispersive with a phase speed proportional to the peak mean longshore current, $c \sim 0.5 - 0.7\, V_{max}$. Their period and wavelength in natural beaches are

[1] *Departament de Física Aplicada, Universitat Politècnica de Catalunya, 08034 Barcelona, Spain*

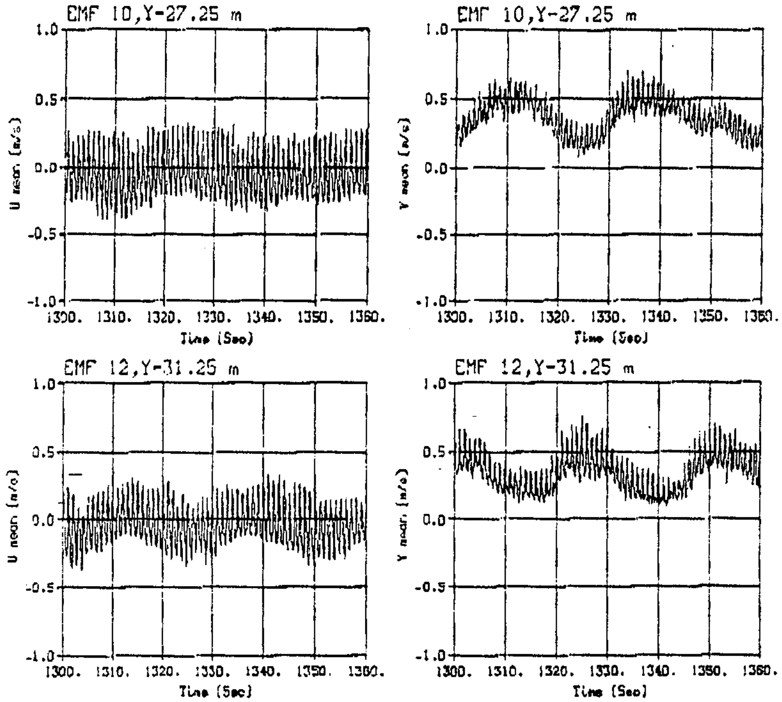

Figure 1: Time series of cross-shore (left) and longshore (right) components of the current at two alongshore locations. LIP experiment M19, from Reniers et al. 1994.

of the order of 10^2 sec. and 10^2 m. respectively. More recently, experiments have been conducted in a wave basin (Delft Hydraulics facilities, LIP project M19) in order to observe FIG waves in a laboratory beach. Preliminary analysis of data in the case of a barred beach profile (Reniers et al., 1994) indicates the presence of FIG waves of a period and a wavelength of about 25 sec. and 8 m. respectively. Time series of alongshore and cross-shore components of the current for two different current-meters in two different alongshore positions are shown in Fig.1. The incoming waves of a period of 1 sec. and strong low frequency oscillations with a period of about 25 sec. may be seen. The amplitude of these oscillations in comparison with the peak longshore current is of the order of 20% for the cross-shore component and 35% for the longshore component. These amplitudes are of the same order of magnitude as those observed by Oltman-Shay et al. (1989) at Duck (USA).

Bowen and Holman (1989) proposed a theoretical explanation for the FIG waves based on an instability mechanism of the mean longshore current. According to their theory, the longshore current may be unstable because of the shear and this instability may generate growing disturbances that progress downflow or shear waves. Their theory was developed using a very simplified analytical model that succeded in giving the main features of the instability and matched the experimental results of Oltman-Shay et al. reasonably well. Nevertheless, their model has a number of limitations such as unrealistic geometry, inviscid flow, rigid lid and linearized governing equations and several improvements are therefore necessary in order to analyze the instability mechanism in more realistic conditions. This has been done by Dodd et al. (1992), Putrevu and Svendsen (1992), Deguchi et al. (1992), Dodd (1994), Dodd and Thornton (1992) and Falqués and Iranzo (1994).

The first aim of the present contribution is to find general transition conditions for shear instability as a function of some non-dimensional parameters involving the longshore current, the topography of the beach, the bottom friction and the lateral mixing. The second aim is to show how the linear stability analysis can be applied to any particular beach, handling actual cross-shore profiles of longshore current, bathymetry, bottom friction and eddy viscosity. Furthermore, the linear analysis can explain the initial growth and propagation of small amplitude shear waves but cannot describe properly the finite amplitude shear waves actually observed in Nature. In particular, the linear theory cannot predict the amplitude of such shear waves. This requires a nonlinear stability analysis which is our third goal.

The importance of shear instability lies in several factors. The theoretical models for the longshore current are usually based on an equilibrium between the driving forces from the incoming wave field and dissipative forces from bottom friction and lateral mixing. But the possibility of instability in such an equilibrium solution indicates that the matter is not so simple and that in some cases the longshore current may have a dynamic behaviour quite far from this equilibrium. Moreover, as several authors have pointed out (see Putrevu and Svendsen, 1992) shear instability can be a mixing factor in the surf zone which is quite stronger than the mixing due to wave induced turbulence.

2. Linear Analysis

We consider the shallow water equations for momentum and mass conservation with a lateral momentum diffusion given by $\nu(x)$:

$$\frac{\partial v_i}{\partial t} + v_j v_{i,j} + g\eta_{,i} = -\frac{c_d}{\zeta}|\vec{v}|v_i + \frac{1}{\zeta}S_{ij,j} + \frac{1}{\zeta}[\nu\zeta(v_{i,j} + v_{j,i})]_{,j} \qquad i = 1,2 \tag{1}$$

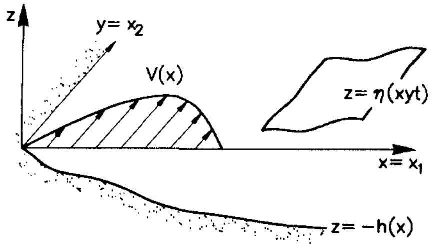

Figure 2: Coordinate system and geometry.

$$\frac{\partial \eta}{\partial t} + [\zeta v_j]_{,j} = 0 \tag{2}$$

Here, $x = x_1$ and $y = x_2$ are the cross-shore and long-shore coordinates (see Fig.2) and repeated indexes are assumed to be summed. The derivative with respect to x_i has been indicated by the subindex $,i$. The total depth is $\zeta = \eta + h$, where $h(x)$ stands for the still water depth and $\eta(x, y, t)$ for the free surface elevation. We assume a quadratic bottom friction with a $c_d(x)$ coefficient and S_{ij} are the radiation stresses.

We consider a basic undisturbed state which is a steady solution of equations (1)-(2) given by $v_1 = 0, v_2 = V(x), \eta = \bar{\eta}(x)$, where $V(x)$ is the longshore current and $\bar{\eta}(x)$ the wave set up/down. Then we superpose on the basic flow a small perturbation of the form

$$e^{ik(y-ct)}(u(x), v(x), \eta(x))$$

and upon linearization of the shallow water equations, (1)-(2), we obtain the eigenproblem:

$$ik(V-c)u + c_d V u + g\eta_x =$$

$$2\nu_x u_x + \nu(2u_{xx} - k^2 u + ikv_x + 2\frac{\bar{\zeta}_x}{H}u_x + ik\frac{V_x}{\bar{\zeta}}\eta) \tag{3a}$$

$$V_x u + ik(V-c)v + 2c_d V v + ikg\eta =$$

$$\nu_x(v_x + iku) + \nu(v_{xx} - 2k^2 v + iku_x - \frac{\bar{\zeta}_x V_x}{\bar{\zeta}^2}\eta + \frac{V_x}{\bar{\zeta}}\eta_x + \frac{\bar{\zeta}_x}{\bar{\zeta}}(v_x + iku)) \tag{3b}$$

$$(\bar{\zeta}u)_x + ik\bar{\zeta}v + ik(V-c)\eta = 0 \tag{3c}$$

where the subindex x indicates differentiation with respect to x. The eigenvalue, $c = \omega/k = (\omega_r + i\omega_i)/k$, is the phase speed, which may be complex. The period and the wavelength are given by $T = 2\pi/\omega_r$ and $\lambda = 2\pi/k$. The total depth is given by $\bar{\zeta} = h(x) + \bar{\eta}(x)$. In these linearized equations any perturbation in the radiation stresses has been neglected.

Given any set of current, bathymetry, bottom friction and viscosity profiles, and for any wavenumber, k, Equations (3) can be solved numerically by using spectral expansions. The details of the numerical procedure can be seen in Falqués and Iranzo (1992, 1994) or Iranzo and Falqués (1992). In that way the $k-\omega_r$ and the $k-\omega_i$ curves, that is, the dispersion and the instability curves can be computed. The basic flow is unstable if there is some wavenumber with positive growthrate, $\omega_i > 0$, and stable otherwise. The fastest growing wavelength in the linear theory, FGM, can be determined as the maximum in the $k-\omega_i$ curve. Although shear waves observed in experiments have a finite amplitude and therefore need a nonlinear analysis, this wavelength, and its corresponding period that can be obtained from the dispersion line, are expected to give some estimate of the observed wavelength and period. This kind of analysis is presented here in two different ways: i) using analitical profiles to find general properties of shear instability, ii) using measured profiles for some particular beach.

The motivation for the first aim is as follows. For many Fluid Mechanics stability problems such as Rayleigh-Bénard convection and Couette flow, there are non-dimensional parameters say Reynolds number, Rayleigh number, etc. governing the transition between stability and instability and the sequence of bifurcations arising from the basic flow (Drazin and Reid, 1981). So far, transition conditions as a function of non-dimensional parameters have been lacking for shear instability of the longshore current. The latter stability problem has two dissipative sources, namely, bottom friction and eddy viscosity, which stabilize the flow. Our aim is to find two non-dimensional parameters related to bottom friction, viscosity, the current and the topography that govern stability. In such a way, transition lines in the plane of both parameters will be obtained and these lines will allow for a rough prediction of stability or instability for a wide class of beaches. For this purpose we will consider a basic current profile given by

$$V(x) = ax\,exp(-(bx)^3) \tag{4}$$

This profile was suggested by Bowen and Holman (1989) and used by Falqués and Iranzo (1994). It can be an equilibrium solution of Equations 1-2 for a suitable radiation stress distribution. The parameters a, b are related to the maximum backshear and to the width of the current trough $l_0 = 0.69/b$ and $f_s = 0.79a$ where l_0 is the offshore distance of the peak of the current and f_s is the maximum backshear, that is, the maximum shear at the sea-face of the current profile. Many realistic current profiles can be roughly fitted by (4) for suitable values of a and b. Concerning topography, we will consider the most simple situation, that is, plane sloping beach. Also, we will neglect the wave set-up/down which, regarding stability analysis, gives just a small correction on the total depth, $\bar{\zeta}(x)$. These simplifications allow us to handle only one parameter related to the bathymetry which is the beach slope, β. So, we assume

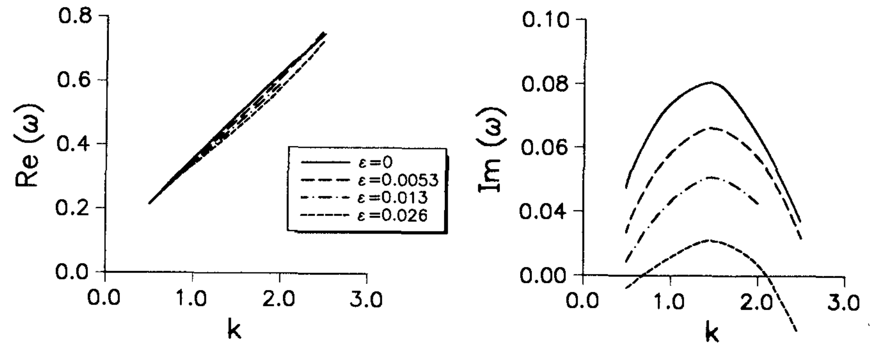

Figure 3: Dispersion (left) and instability (right) curves for $F = 0.3, c_d = 0, x_b/l_0 = 1.6, \alpha l_0 = 3.5$ and for several maximum eddy viscosities.

$\bar{\zeta}(x) = h(x) = \beta x$. Concerning lateral mixing, we consider (see Deguchi et al., 1992)

$$\nu(x) = \nu_m (h(x)/h(x_b))^{3/2} \quad if \quad x \leq x_b \tag{5a}$$

$$\nu(x) = \nu_m e^{-\alpha(x-x_b)} \quad if \quad x \geq x_b \tag{5b}$$

Finally, a uniform bottom friction coefficient, c_d, has been assumed. Equations (3) have been scaled using the cross-shore lengthscale of the current and its maximum backshear in such a way that we have taken $b^{-1} = 1.45 l_0$ as lengthscale and $a^{-1} = 0.79 f_s^{-1}$ as timescale. After this scaling the non-dimensional parameters in the equations are the maximum Froude number of the basic flow, $F = (V(x)/\sqrt{gh(x)})_{max} = 0.63a/\sqrt{\beta g b}$, the frictional parameter, c_d/β, and the non-dimensional maximum eddy viscosity, $\epsilon = \nu_m / f_s l_0^2$, which plays the role of a reciprocal Reynolds number, Re^{-1}. Concerning lateral mixing, two more parameters appear: the position of the maximum viscosity in comparison with the maximum in the current, x_b/l_0, and the non-dimensional offshore gradient, αl_0.

Typical instability and dispersion lines are shown in Figure 3 for increasing viscosity from $\epsilon = 0$ up to $\epsilon = 0.026$, with no bottom friction and for $F = 0.3$. The wavenumber k, and the complex frequency ω have been scaled to b and a. In accordance with previous work, the dispersion relations are quite linear. The general trends we have found are that increasing bottom friction and/or eddy viscosity results in a decrease in growthrates, ω_i, and in a small decrease in frequencies. An increase in Froude number decreases instability too. This may be because for high Froude number shear instability feeds surface gravity modes so that instability is weakened. These general characteristics may have some exception regarding viscosity. When the eddy viscosity distribution has its maximum around the maximum in the current profile and has a strong offshore decay (large α) an increase in eddy viscosity can result in a larger growthrate. If ϵ goes on increasing, this trend is reversed and stability is finally reached. This behaviour can be understood by considering that viscosity has two opposite effects: it dampes instability but also has a diffusive effect which propagates perturbations and therefore favours instability. Then, when ν_m increases from a very small value the viscosity in the sea face of the current profile still remains negligible at the beginning, whereas it reaches significant values at the shore face of the profile. Since the source of the instability is mainly located in the sea face (in the region where the backshear is maximum) the damping effect is therefore negligible. On the other hand, the diffusive effects at the shore face can be important. If ν_m continues to increase, the values of $\nu(x)$ near the maximum backshear become large enough so that the damping effect become dominant. This is in contrast with the effects from bottom friction. Dodd (1994) found that there may be destabilizing effects due to bottom friction (curvature terms) but that the overall effect was a stabilizing one. In line with his results, we also find that the overall influence of bottom friction on shear instability is always a stabilizing one.

In any case, for each set of values of $F, x_b/l_0, \alpha l_0$ and for each c_d/β we find a critical value of ϵ such that instability requieres lower values. We thus obtain a stability diagram in the $\epsilon - c_d/\beta$ plane with transition lines that bound stability and instability regions. These lines are shown in Fig.4 for $F = 0.14, F = 0.3$ and $F = 0.89$. We have set $x_b/l_0 = 1.6$ and $\alpha l_0 = 3.5$. Very small sensitivity has been observed to the latter two parameters, except for the case $x_b/l_0 \simeq 1$ and large αl_0 described above, which is not very realistic because x_b is usually expected to be offshore of the maximum in the current. As can be seen in Fig.4, for small Froude number instability is almost insensitive to Froude number. However, for high values some sensitivity appears and the stability region is widened.

Some experimental data sets have also been plotted in Fig. 4. This is not an easy job as only crude estimates of c_d, ν are available, the actual current profiles are usually rather far from (4) even for suitable a, b and we have to rely on a mean beach slope, β. Though these limitations result in large error bar we think that the diagram can be useful in giving a rough prediction of stability or instability. Four data sets have been represented: Duck (USA), Leadbetter (USA), wave-basin experiment (LIP project M19, The Netherlands) and Trabucador (Ebro Delta, Spain). The experimental information was taken from Dodd et al. (1992), Reniers et al. (1994) and Redondo et al. (1994). The lateral mixing was estimated according to Deguchi et al. (1992). The most stable situation corresponds to Leadbetter beach and indeed no evidence of shear waves was found at this site. On the other hand, the diagram predicts

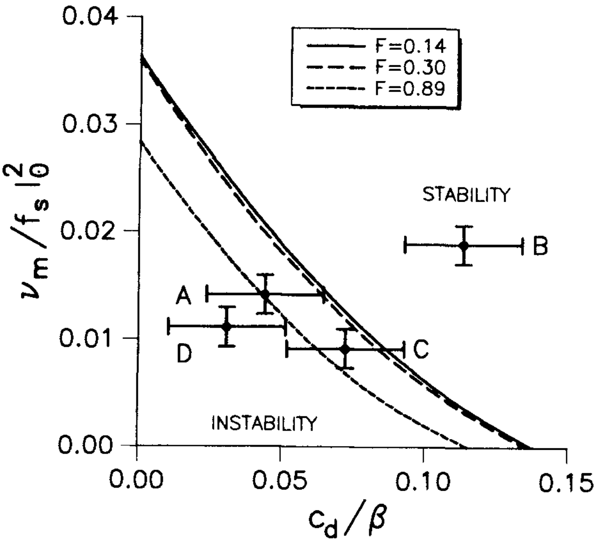

Figure 4: Transition lines for $x_b/l_0 = 1.6, \alpha l_0 = 3.5$ and for three Froude numbers. Four experimental data sets have also been plotted: A:Duck (USA); B:Leadbetter (USA); C:Wave-basin experiment LIP project M19; D:Trabucador (Spain).

instability for Duck data set in agreement with observations (the maximum Froude number did not exceed 0.3). The Trabucador data set also leads to instability according to the model. A complete data analysis is not yet available (Delta'93 campaign). However, a preliminary inspection indicates the presence of low frequency oscilations that might be shear waves. Regarding the wave basin experiment, the maximum Froude number reached $F = 0.7$, so the corresponding box in the diagram would match the transition line that would be somewhere in between the $F = 0.3$ and the $F = 0.89$ lines. Therefore, no conclusive analysis can be made by this way in this case and a detailed numerical simulation for the actual $V(x), \bar{\zeta}(x), c_d(x)$ and $\nu(x)$ profiles is necessary. In any case, if we want a more accurate prediction of instability, with the period and wavelength of the shear waves, this computation for the actual profiles is needed. This kind of analysis has been made for Trabucador Beach, and for the wave basin experiment. Although a detailed analysis of the results of this latter experiment is under way, some preliminary results are already available. For instance, measurements from the longshore array of currentmeters for one of the tests with barred beach indicated the presence of shear waves with a period of approximately $25sec.$ and a phase speed of $0.33m/s$, giving rise to a wavelength of $8.3m$. In this case, a dominant mode with a wavelength of $2\pi/k = 7.3m$ and a period of $2\pi/\omega_r = 27sec.$ was obtained from the numerical model. Experiments and theory were thus found to be in a fairly good agreement.

3. Nonlinear Stability

Only a preliminary study of the nonlinear shear instability is currently available, and a much more detailed analysis is under way. For this preliminary study, some assumptions have been made: plane sloping topography, uniform bottom friction and viscosity coefficients, a basic current given by (4) and the rigid lid assumption, that is, the vertical fluxes are much smaller than the horizontal ones (Bowen and Holman, 1989). Falqués and Iranzo (1994) showed that rigid lid hypothesis was a suitable one for low Froude number so that for F up to 0.6 only a correction less than 12% was necessary in growthrates. Therefore, rigid lid assumption is not a severe restriction for natural beaches. A further assumption regarding the mean flux that will be specified later on has been taken into account. The mass conservation equation (2) and the rigid lid hypothesis allow us to use a streamfunction for the perturbation, $\psi(x, y, t)$, defined by:

$$v_1 = \frac{1}{h}\frac{\partial\psi}{\partial y} \quad , \quad v_2 = V(x) - \frac{1}{h}\frac{\partial\psi}{\partial x} \tag{6}$$

Then, by taking the curl of the momentum equations (1) we end-up with a single governing equation which is

$$\mathcal{C}\frac{\partial\psi}{\partial t} = \mathcal{M}\psi + \mathcal{N}(\psi) \tag{7}$$

where the linear operators $\mathcal{C}$ and $\mathcal{M}$ are given by

$$\mathcal{C}\psi = \frac{1}{h}(\frac{h_x}{h}\psi_x - \Delta\psi)$$

$$\mathcal{M}\psi = -V\mathcal{C}\psi_y + \psi_y\mathcal{C}V + \frac{c_d V}{h^2}(2\psi_{xx} + \psi_{yy} + 2(\frac{V_x}{V} - 2\frac{h_x}{h})\psi_x) +$$
$$+\nu((\frac{h_x}{h})_x(\mathcal{C}\psi + \frac{2}{h}\psi_{yy}) + \frac{h_x}{h}(\mathcal{C}\psi)_x + \Delta(\mathcal{C}\psi))$$

and the nonlinear operator $\mathcal{N}$ is given by

$$\mathcal{N}(\psi) = \frac{1}{h}(\psi_x\mathcal{C}\psi_y - \psi_y(\mathcal{C}\psi)_x + \frac{h_x}{h}\psi_y\mathcal{C}\psi)$$

The subindices x, y mean derivative with respect to x or y and the operator Δ is the 2D horizontal Laplace operator. The operator $\mathcal{C}$ applied to ψ gives the vertical component of the vorticity. Hereafter, the scaling introduced in Section 2 is used. Equation (7) has to be solved in the domain $x, y \in (0, +\infty)$ x $(-\infty, +\infty)$. However, for technical reasons the cross-shore domain has been cut off at some suitable offshore position, $x = l$. A comparison between the spectrum of the linear part of (7) and the spectrum of (3) solved without this restriction shows that the error remains very small if l is large enough compared to the width of the current. A suitable value has been $l = 6$. The boundary conditions at the shoreline and far offshore are:

$$\psi = \psi_x = 0 \qquad x = 0, x = l \tag{8}$$

Periodicity conditions with respect to some basic wavelength, $\lambda_0 = 2\pi/K_0$, have been used as boundary conditions regarding the longshore coordinate. The boundary conditions at $x = l$ just mean vanishing cross-shore and longshore velocity perturbations far offshore. Concerning the shoreline the matter is not so simple because of the singularity coming from $h(0) = 0$. The set of boundary conditions chosen at $x = 0$ ensures a bounded velocity field at the shoreline and it means vanishing mass transport.

Equation (7) has been solved numerically using a spectral Chebyshev-Fourier expansion

$$\psi(x,y,t) = \sum_{k=-n}^{k=n-1} \sum_{j=0}^{m} a_{kj}(t) T_j(x) e^{ikK_o y} \tag{9}$$

where $T_j(x)$ are Chebyshev polynomials. After spatial discretization which is performed by Galerkin projection concerning y and by collocation concerning x, Equation (7) reads as a set of $2n$ vector ordinary differential equations (one for each alongshore Fourier mode)

$$\hat{\mathcal{C}}_k \frac{d\vec{a}_k}{dt} = \hat{\mathcal{M}}_k \vec{a}_k + \vec{\mathcal{N}}_k(\vec{a}_{-n}...\vec{a}_0...\vec{a}_{n-1}) \qquad k = -n, ..., n-1 \tag{10}$$

where the $(m+1)$x$(m+1)$ matrices $\hat{\mathcal{C}}_k, \hat{\mathcal{M}}_k$ and the vector functions $\vec{\mathcal{N}}_k$ are the discrete versions of operators $\mathcal{C}, \mathcal{M}, \mathcal{N}$ for each Fourier mode, k, and where $\vec{a}_k = (a_{0k}, a_{1k}, ...a_{mk})$ stands for the $m+1$ Chebyshev coefficients of the Fourier mode k. The equations corresponding to each Fourier mode are coupled only because of their nonlinear terms, $\vec{\mathcal{N}}_k$. Time discretization proceeds by using a semi-implicit Euler scheme

$$(\hat{\mathcal{C}}_k - \delta t\, \hat{\mathcal{M}}_k)\vec{a}_k^{\tau+1} = \hat{\mathcal{C}}_k \vec{a}_k^{\tau} + \delta t\, \vec{\mathcal{N}}_k(\vec{a}_{-n}^{\tau}...\vec{a}_{n-1}^{\tau}) \qquad k = -n, ..., n-1 \tag{11}$$

Given the solution $\vec{a}_k^{\tau}$ at time step τ, Eq.11 is linear in $\vec{a}_k^{\tau+1}$ and can be easily solved. More details and references on numerical spectral methods applied to coastal dynamics may be seen in Falqués and Iranzo, (1992, 1994) or in Iranzo and Falqués (1992).

Some sensitivity tests concerning the parameters of the numerical model were made. The model proved to be quite robust and the values of $m = 40, n = 8, \delta t = 0.01$ were found to be suitable for the preliminary study made up to

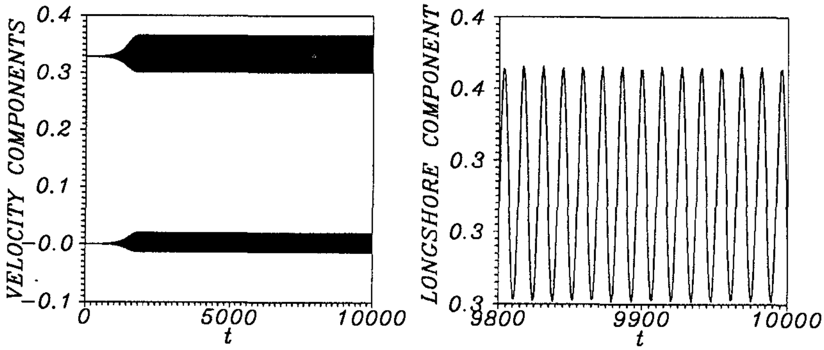

Figure 5: Time evolution from a small initial perturbation for $\epsilon = 0.053, \mu = 11.1$. Time series of cross-shore and longshore velocity components (left) and final steady oscillation in the longshore component (right).

now. Owing to the linear theory outlined in Section 2 the control parameters for instability are the frictional parameter, $\mu = \beta/c_d$, and the non-dimensional viscosity, $\epsilon = \nu_m/f_s l_0^2$. Time evolution from some initial perturbations has been computed for several values of ϵ, μ. For any ϵ, a critical value μ_c was found to exist such that below it all the perturbations tend to vanish whereas above it the perturbations grow. At the beginning this growth is nearly exponential but then a saturation is reached and a final oscillatory solution is obtained. For μ slightly higher than μ_c its period is very close to the period predicted for the linear theory. The critical value, μ_c, coincides with that given by the linear analysis. For instance, for $\epsilon = 0.053$ the transition occurs at $\mu_c = 10.0$. One test slighly above critical conditions ($\mu = 11.1$) is shown in Fig. 5. These results show that shear instability of the longshore current gives rise to a supercritical Hopf bifurcation and are in line with the weakly nonlinear analysis carried out by Dodd and Thornton (1992). Far from criticality the behaviour may be quite complicated: an energy transfer between Fourier modes occurs, the FGM mode may be no longer dominant, the final steady wave may be modulated... A further increase in μ leads to a blow-up of the numerical model. For $\epsilon = 0.053$ this occurs for $\mu > 20$ and may be due to numerical instabilities that might be due in turn to a further bifurcation in the physical problem. This is currently being investigated. An example of the strongly nonlinear behaviour is shown in Figure 6 by means of a time evolution from a small initial perturbation for $\epsilon = 0.053, \mu = 20$. In this test, the basic wavenumber has been chosen to be $K_0 = 0.467$, that is, one third of the FGM (linearly dominant) which is 1.4. This means that the FGM mode corresponds to $k = 3$ so that the simulation uses two subharmonics in addition to the superharmonics. As we can see, the first mode to grow significantly is $k = 3$. Apparently, it reaches a saturation.

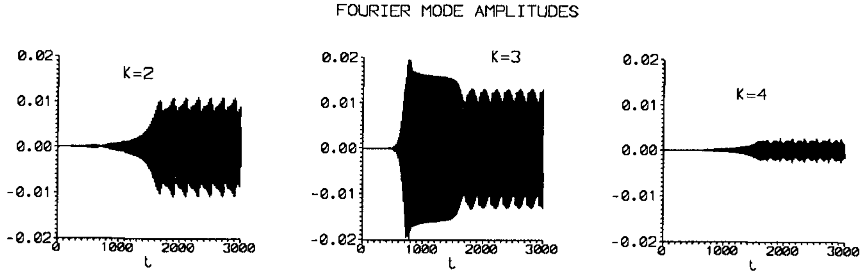

Figure 6: Time evolution of the FGM, $k = 3$, its subharmonic $k = 2$ and its superharmonic $k = 4$ from a small initial perturbation for $\epsilon = 0.053, \mu = 20$. The basic wavenumber is $K_0 = 0.467$.

However, it slowly looses part of its energy by feeding the other modes, specially the $k = 2$ subharmonic and the $k = 0$ mode. Finally, the other modes reach a saturation and a final steady modulated oscillation in all modes starts. The time unit in all these plots is the timescale defined in Section 2 and based on the maximum backshear of the basic flow. For natural beaches, 10 units may be of the order of $1min$. Therefore, our numerical time series of 10000 time units would represent a real time of 16 hours. This is quite enough for shear wave simulation.

According to the numerical experiments performed some preliminary properties of finite amplitude shear waves can be summarized. For each set of values of μ, ϵ the final finite amplitude shear waves has been computed from several initial conditions and no sensitivity to the initial conditions has been found except in the parameters range where the numerical model blows up. As expected, the flow pattern corresponding to the perturbation for near critical conditions is very similar to the linear eigenfunction although some asymmetry between crests and troughs can be noticed. However, far from criticality the streamlines are quite different from the linear ones, showing a strong mean flow component (Fig. 7). This component comes from the 0 Fourier mode and means a correction on the mean flow due to the instability. Because of the boundary conditions at the shoreline (8) the mean alongshore discharge due to the perturbation vanishes, $\psi(l, y, t) - \psi(0, y, t) = 0$. This is an unphysical constraint on the mean flow and has been taken because of technical reasons concerning the boundary conditions and the numerical procedures. Work is under way in order to relax this constraint by considering boundary conditions (8) only for $k \neq 0$. However, the present results already suggest that the mean flow component of the perturbation is not very important for near critical

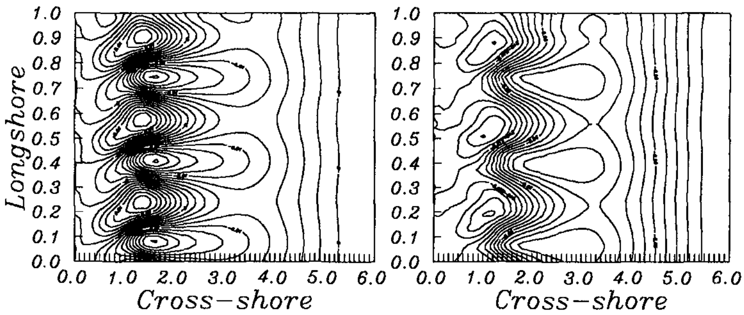

Figure 7: Streamlines of the perturbation, (A): near critical conditions ($\epsilon = 0.053, \mu = 11.1$), (B): strongly nonlinear ($\epsilon = 0.053, \mu = 20.0$).

conditions but can have a strong influence far from criticality. The amplitude of shear waves can be defined, for instance, as the fluctuation in the cross-shore component in comparison with the mean longshore current. This ratio has been plotted in Figure 8 as a function of the control parameter μ for $\epsilon = 0.053$. This provides us with a bifurcation diagram for shear instability. Notice that this amplitude can reach 20%, that is, the same order of magnitude as the amplitudes measured at Duck (Oltman-Shay et al., 1989) or in the LIP experiment (Reniers et al., 1994). This is in contrast with the weakly nonlinear analysis of Dodd and Thornton (1992), where only amplitudes of about 0.07% were obtained. The curve stops when the numerical model breaks down. Intriguingly, this occurs roughly when the amplitude of shear waves reaches the maximum value observed in experiments, $u/V_{max} \sim 0.2$. The relationship between the final amplitude and the linear growthrate is shown in Figure 9. In qualitative agreement with the weakly nonlinear theory a small nonlinear correction on the period of the shear waves has been found. The relative increase, shown in Figure 9, can reach 6%.

4. Conclusions

Analytical profiles for the current, eddy viscosity and bottom friction coefficient, and a mean beach slope have been used to investigate the general trends for shear instability of the longshore current. The overall influence of bottom friction and lateral mixing is a stabilizing effect and a small decrease in the frequency of shear waves. However, for some eddy viscosity profiles this trend is not monotone and an increase in viscosity may eventually result in

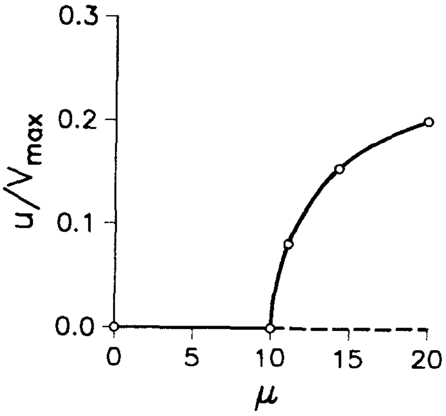

Figure 8: Bifurcation curve showing the amplitude of the crossshore fluctuation in the current with respect to the mean longshore current for $\epsilon = 0.053$.

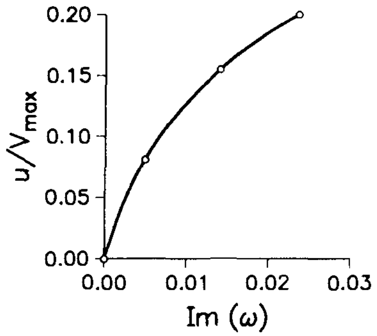

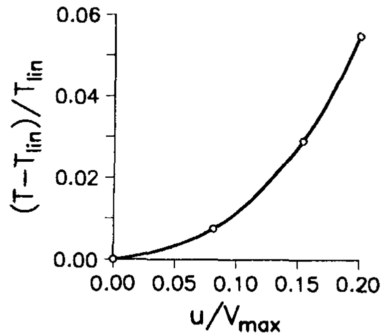

Figure 9: Left: amplitude of the final shear wave as a function of the linear growthrate. Right: Relative increase in the period of the shear wave as a function of the amplitude.($\epsilon = 0.053$).

larger growthrates. An instability diagram as a function of two non-dimensional parameters related to bottom friction, lateral mixing, the current and the bathymetry has been presented. This diagram allows for a rough prediction of shear stability characteristics for any beach and has been found to compare fairly well with four experimental data sets. A more accurate study of shear instability for a given situation requires the use of the actual profiles. This has been done for a wave basin experiment and a good agreement between numerical modelling and measurements has been found. A nonlinear numerical simulation has also been conducted. In accordance with the weakly nonlinear theory (Dodd and Thornton, 1992) shear instability has been found to give finite amplitude waves through a supercritical Hopf bifurcation. However, the amplitudes are larger than the weakly nonlinear ones and reach at least 20% of the mean current. A small nonlinear correction on the period has also been found. Far from critical conditions shear waves can exhibit a complicated behaviour, with a modulation and with a flow pattern rather different from that predicted by the linear theory. Preliminary results suggest that for the strongly nonlinear situation there can be an important contribution of instability to the mean current.

References

Bowen A.J. and Holman R.A., 1989. *Shear instabilities of the mean longshore current, 1. Theory*, J.Geophys.Res. 94, C12, 18023-18030.

Deguchi I., Sawaragi T. and Ono M., 1992. *Longshore current and lateral mixing in the surf zone.* Proc.23th Int.Conf.Coastal Eng., 202, p.2642-2654.

Dodd N., Oltman-Shay J. and Thornton E.B., 1992. *Shear instabilities in the longshore current: a comparison of observations and theory*, J.Phys.Oceanog. 22, 1 , 62-82.

Dodd N. and Thornton E.B., 1992. *Longshore current instabilities: growth to finite amplitude.* Proc.23th Int.Conf.Coastal Eng., 203, p.2655-2668.

Dodd N., 1994. *On the destabilization of a longshore current on a plane beach: Bottom shear stress, critical conditions, and onset of instability*, J.Geophys.Res., 99, C1, 811-824.

Drazin P.G. and Reid W.H., 1981. *Hydrodynamic Stability.* Cambridge University Press.

Falqués A. and Iranzo I., 1992. *Edge waves on a longshore shear flow*, Phys.Fluids A, 4 (10), 2169-2190.

Falqués A. and Iranzo I., 1994. *Numerical simulation of vorticity waves in the near-shore*, J.Geophys.Res., 99, C1, 825-841.

Iranzo V. and Falqués A., 1992. *Some spectral approximations for differential equations in unbounded domains*, Comp.Meth.Appl. Mech.Eng., 98, 105-126.

Oltman-Shay J., Howd P.A.and Birkemeier W.A., 1989. *Shear instabilities of the mean longshore current, 2. Field observations*, J.Geophys.Res. 94, C12, 18031-18042.

Putrevu U. and Svendsen I.A.,1992. *Shear instability of longshore currents: A numerical study*, J.Geophys.Res. 97, C5, 7283-7303.

Redondo J.M., Rodriguez A., Bahia E., Falqués A., Gracia V., Sánchez-Arcilla A. and Stive M.J.F., 1994. *Image analysis of surf zone hydrodynamics*, Coastal Dynamics'94, p.350-365.

Reniers A.J., Battjes J.A., Falqués A. and Huntley D.A., 1994. *Shear-wave laboratory experiment*, Proc.Int.Symposium: waves – physical and numerical modelling, vo.1, 356-365.